

Fingerprint classification combined with Gabor filter and convolutional neural network



Zhengfang He^{1,2,*}, Ivy Kim D. Machica¹, Jan Carlo T. Arroyo^{3,4}, Ma. Luche P. Sabayle⁵, Weibin Su^{1,2}, Gang Xu^{1,2}, Yikai Wang², Mingbo Pan², Allemar Jhone P. Delima³

¹College of Information and Computing, University of Southeastern Philippines, Davao City, Davao del Sur, Philippines

²School of Intelligent Science and Engineering, Yunnan Technology and Business University, Kunming, China

³College of Information and Computing Studies, Northern Iloilo State University, Estancia, Iloilo, Philippines

⁴College of Computing Education, University of Mindanao, Davao City, Davao del Sur, Philippines

⁵College of Information and Communications Technology, West Visayas State University, Iloilo City, Philippines

ARTICLE INFO

Article history:

Received 25 May 2022

Received in revised form

2 September 2022

Accepted 24 September 2022

Keywords:

Convolutional neural network

Fingerprint classification

Gabor filter

Image enhancement

ABSTRACT

A fingerprint is an impression left by the friction ridges of a human finger. A fingerprint classification system groups fingerprint according to their characteristics and therefore helps to match a fingerprint against an extensive database of fingerprints. The Henry classification system is widely used among fingerprint classification systems. Some researchers have used traditional machine learning or deep learning for fingerprint classification. Nevertheless, traditional algorithms cannot extract the depth features of the fingerprint, and most deep learning algorithms lack fingerprint image enhancement. So, this paper combined the Gabor Filter and Convolutional Neural Network to extract fingerprint features. The model has two channels, one is a Deep Convolutional Neural Network (DCNN), and the other is a Shallow Convolutional Neural Network (SCNN). The DCNN consists of a neural network with eight layers, which can extract deep features of the fingerprint. The SCNN consists of Gabor Filter and a neural network with two layers that can extract features from clear fingerprint images. This paper uses NIST Special Database 4 for experiments. Experimental results show that the model proposed in this paper has achieved 91.4% accuracy. Compared with other algorithms, this model has higher accuracy than others. It shows that combined with the Gabor Filter and Convolutional Neural Network can better extract the ridge features of fingerprint images.

© 2022 The Authors. Published by IASE. This is an open access article under the CC BY-NC-ND license (<http://creativecommons.org/licenses/by-nc-nd/4.0/>).

1. Introduction

A fingerprint is an impression left by the friction ridges of a human finger. Recovering partial fingerprints from a crime scene is an important method of forensic science. Moisture and grease on a finger result in fingerprints on surfaces such as glass or metal. Deliberate impressions of entire fingerprints can be obtained by ink or other substances transferred from the peaks of friction ridges on the skin to a smooth surface such as paper. Fingerprint records normally contain impressions from the pad on the last joint of the fingers and thumbs (Zhengfang et al., 2022).

A fingerprint classification system groups fingerprint according to their characteristics and therefore helps to match a fingerprint against a large database of fingerprints. A query fingerprint that needs to be matched can therefore be compared with a subset of fingerprints in an existing database (Li and Jain, 2015).

Early classification systems were based on the general ridge patterns, including the presence or absence of circular patterns of several or all fingers. This allowed the filing and retrieval of paper records in large collections based on friction ridge patterns alone. The most popular systems used the pattern class of each finger to form a numeric key to assist lookup in a filing system (Moenssens, 1971; Karu and Jain, 1996; Yager and Amin, 2004). Among fingerprint classification systems, the Henry classification system is widely used (Jiang, 2015).

In the early 1890s, British fingerprint scientist Edward Henry established the famous Henry fingerprint classification system. Edward Henry

* Corresponding Author.

Email Address: hfrommane@qq.com (Z. He)

<https://doi.org/10.21833/ijaas.2023.01.010>

Corresponding author's ORCID profile:

<https://orcid.org/0000-0002-8075-4122>

2313-626X/© 2022 The Authors. Published by IASE.

This is an open access article under the CC BY-NC-ND license

(<http://creativecommons.org/licenses/by-nc-nd/4.0/>)

divided fingerprints into five types for the first time: Right Loop, Left Loop, Whorl, Arch, and Tented Arch

(Faulds, 1880). These five types are shown in Fig. 1.

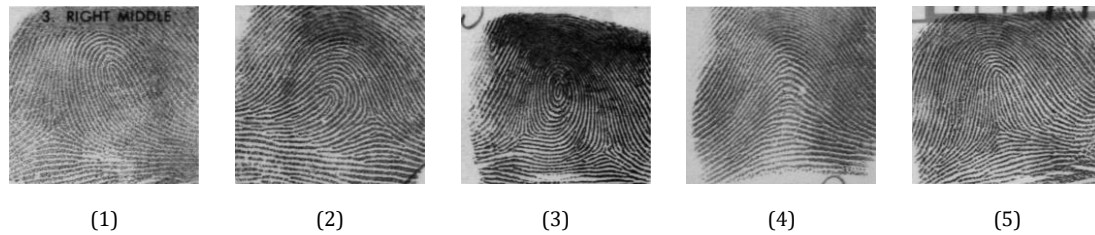


Fig. 1: Examples of fingerprints from each class of the Henry System for fingerprint classification; (1) Right loop; (2) Left loop; (3) Whorl; (4) Arch; and (5) Tented arch

At present, the existing fingerprint classification algorithms are based on one or more of the following features: Ridge Line Flows (Chang and Fan, 2002; Cao et al., 2013), Orientation Field, Singular Point (Wang et al., 2009; Cao et al., 2013; Guo et al., 2014), and Gabor filter (Leung and Leung, 2010).

2. Review of related literature

In the traditional fingerprint classification algorithms, Ding et al. (2020) proposed the Twin Support Vector Machine (TWSVM) model. First, the Gabor filter extracts texture features from fingerprint images. Second, a multi-class model based on TWSVM is constructed. The quantum particle swarm optimization algorithm is used to optimize the parameters in the model. Then the fingerprints are divided into five classes using the optimized model. The experimental results show that applying the TWSVM to fingerprint classification can get good classification results. However, this paper believes that this algorithm cannot extract the depth features of the fingerprint.

Many researchers are using CNN for fingerprint classification. Wu et al. (2020) proposed the FCTP-Net model. This model consists of four convolutional layers, three max-pooling layers, two norm layers, and three fully-connected layers. Experimental tests show that the proposed model can recognize the pattern features from a giant fingerprint database using CNN's automatic learning and feature extraction abilities to get more incredible accuracy. Rim et al. (2021) proposed a classification method to identify detailed fingerprint information using a deep learning model. Five advanced deep learning models such as classic CNN, AlexNet, VGG-16, Yolo-v2, and Resnet-50 were adapted to be trained from scratch. From their experimental results, each of the five models has advantages and disadvantages. However, this paper argues that these models have no fingerprint enhancement and lack the extraction of clear fingerprint features.

Also, many researchers are using CNN to do binary classification tasks. Rim et al. (2020) proposed a deep learning method to automatically and conveniently estimate gender from fingerprints. The VGG-19, ResNet-50, and EfficientNet-B3 models were developed to train from scratch. Their experimental results showed that the EfficientNet-

B3 model achieved the highest accuracy by comparing those advanced models. Ibrahim et al. (2021) proposed an efficient DFCN (deep fingerprint classification network) model to accurately classify real and fake fingerprints. The proposed DFCN achieved high classification performance, where fingerprint images are successfully classified into two categories. Again, this paper argues that these models lack fingerprint enhancement.

Jian et al. (2020) proposed the Lightweight Convolutional Neural Network (LCNN) model based on singularity region of interest (ROI). The experimental results show that the testing set achieves higher accuracy than traditional machine learning algorithms. The LCNN achieves similar performance with fewer parameters than general CNN models. Nevertheless, this paper believes that this algorithm cannot extract the depth features of the fingerprint.

Zia et al. (2019) believed that the softmax probabilities are not an accurate representation of model confidence and often misleading in feature space that may not be represented with the available training samples. Thus, the effectiveness of the fingerprint classification was improved by dealing with false positives using Bayesian model uncertainty. Results show that the accuracy is improved than the traditional DCNN. Also, this paper argues that this model has no fingerprint enhancement.

In summary, traditional algorithms cannot extract the depth features of the fingerprint, and deep learning algorithms lack fingerprint image enhancement. So, this paper combined the Gabor filter and Convolutional Neural Network to extract fingerprint features.

3. Methodology

3.1. Image normalization

Due to the differences in the collection time, light intensity, individual finger pressing force, and the wetness of the finger surface of the fingerprint image collection system, the collected images have significant differences in the distribution of grayscale images. If the grayscale images collected by the same person in different situations are too different, it will increase the difficulty of fingerprint image feature

extraction and matching. Therefore, normalization processing is required after collecting fingerprint images and converting all images into standard images with the given mean and variance. Normalization does not change the friction ridges of the fingerprint, reducing the difference in grayscale values between different fingerprint images.

To normalize the grayscale value of the original input image, the grayscale value of the original image can be adjusted to be within a specific range by normalizing the grayscale range of the original image. A fingerprint image I is defined as a $W \times H$ matrix, where $I(i, j)$ represents the gray value of the pixel in the i -th row and the j -th column. The mean and variance of the fingerprint image I are defined as Eqs. 1 and 2.

$$M(I) = \frac{1}{WH} \sum_{i=0}^{H-1} \sum_{j=0}^{W-1} I(i, j) \quad (1)$$

$$VAR(I) = \sigma^2 = \frac{1}{WH} \sum_{i=0}^{H-1} \sum_{j=0}^{W-1} [I(i, j) - M(I)]^2 \quad (2)$$

The normalized image is G , as shown in Eq. 3.

$$G_{(i,j)} = \begin{cases} M_0 + \sqrt{\frac{\sigma_0^2(I(i,j)-M)^2}{\sigma^2}} & I(i, j) > M \\ M_0 - \sqrt{\frac{\sigma_0^2(I(i,j)-M)^2}{\sigma^2}} & I(i, j) \leq M \end{cases} \quad (3)$$

The $I(i, j)$ and $G_{(i,j)}$ in Eq. 3 are the images before and after normalization, respectively. Moreover, the M_0 and σ_0^2 are the preset average grayscale and mean square error of the image. Furthermore, the M and σ^2 are the grayscale mean and variance of the original image.

3.2. Orientation field estimation

The image orientation is the orientation of the ridge and valley lines in the fingerprint. Rao and Balck (1980) proposed a method to obtain the orientation map using the gradient operator. They used the gray gradient method to calculate the orientation map of the fingerprint image. The main idea of the grayscale gradient method is to calculate the grayscale gradient of each point of the image by using the grayscale changes of the ridge and valley lines of the fingerprint image, and the direction perpendicular to the gradient is the ridge direction of the point. Since the fingerprint is continuous, the Sobel operator (Kanopoulos et al. 1988; Chen et al., 2020) is used.

The normalized image is divided into $W \times W$ pixel blocks. The Sobel operator is then used to calculate the gradient values in the horizontal and vertical directions of each pixel in the block. Fig. 2 shows the Sobel operator template in the x and y directions.

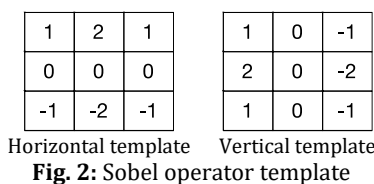


Fig. 2 template is used to convolve the normalized image to get the gradient values in the x and y directions, as shown in Eqs. 4 and 5.

$$V_x(i, j) = \sum_{u=i-\frac{w}{2}}^{i+\frac{w}{2}} \sum_{v=j-\frac{w}{2}}^{j+\frac{w}{2}} 2 \partial_x(u, v) \partial_y(u, v) \quad (4)$$

$$V_y(i, j) = \sum_{u=i-\frac{w}{2}}^{i+\frac{w}{2}} \sum_{v=j-\frac{w}{2}}^{j+\frac{w}{2}} (\partial_x^2(u, v) - \partial_y^2(u, v)) \quad (5)$$

The $V_x(i, j)$ and $V_y(i, j)$ in Eqs. 4 and 5 are the ridge directions in the x and y directions at the center of the pixel (i, j) , respectively. The ∂_x and ∂_y are the gradient values in the x and y directions, and W is the number of blocks. The orientation of each block is calculated using Eq. 6, where θ is the orientation angle of the block.

$$\theta(i, j) = \frac{1}{2} \tan^{-1} \left(\frac{V_x(i, j)}{V_y(i, j)} \right) \quad (6)$$

3.3. Frequency field estimation

In the local non-singular region of the fingerprint image, viewed along the orientation perpendicular to the ridge line, the gray value of the pixel point on the ridge and valley line of the fingerprint roughly forms a two-dimensional sine wave. Define ridge frequency as the reciprocal of the number of pixels between two adjacent peaks or troughs.

After the orientation field is obtained, the gray values of all pixels in each block are projected in their vertical direction. The projection forms a one-dimensional sine wave whose extreme points correspond to the ridges and valleys of the fingerprint. Assuming that $T(i, j)$ is the average number of pixels between two adjacent peaks of the one-dimensional sine wave, the frequency is as shown in Eq. 7.

$$F(i, j) = \frac{1}{T(i, j)} \quad (7)$$

3.4. Gabor filter

Once the orientation and frequency fields of the fingerprint image are determined, these parameters can be used to construct an even-symmetric Gabor filter (Gabor, 1946). Gabor filter is a band-pass filter with direction-selective and frequency-selective properties, and it can achieve the best combination of time and frequency domains. The form of the even symmetric Gabor filter is shown in Eq. 8.

$$G(x, y, \theta, f_0) = \exp \left\{ -\frac{1}{2} \left(\frac{x_\theta^2}{\sigma_x^2} + \frac{y_\theta^2}{\sigma_y^2} \right) \right\} \cos(2\pi f_0 x_\theta) \quad (8)$$

where

$$\begin{bmatrix} x_\theta \\ y_\theta \end{bmatrix} = \begin{bmatrix} \sin \theta & \cos \theta \\ -\cos \theta & \sin \theta \end{bmatrix} \begin{bmatrix} x \\ y \end{bmatrix}$$

In Eq. 8, θ is the direction of the filter, f_0 is the frequency of the ridge, $[x_\theta, y_\theta]$ represents the counterclockwise rotation angle θ of the coordinate

axis $[x,y]$, σ_x and σ_y , are the Gaussian envelope constants for the x and y axes, respectively.

3.5. Convolutional neural network

Convolutional Neural Networks (CNNs) are a powerful class of neural networks primarily designed to process images (Valueva et al., 2020). A

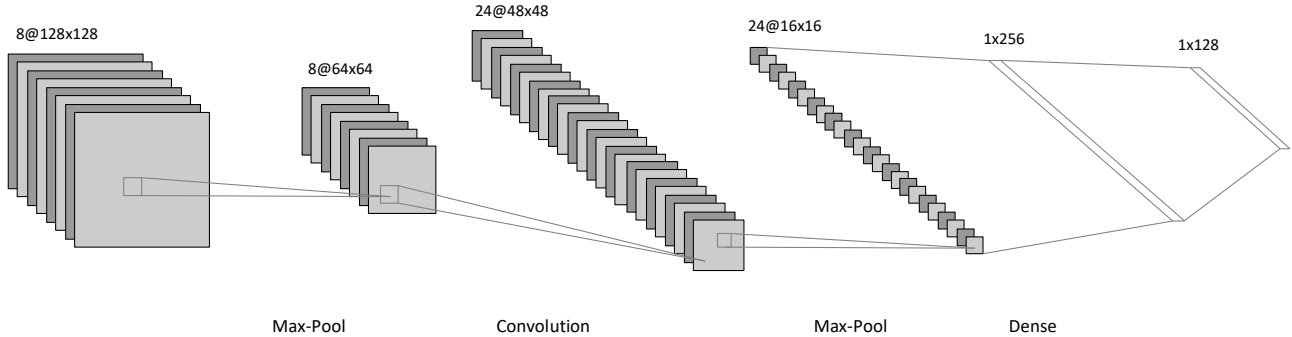


Fig. 3: Typical CNN architecture

Convolutional Neural Networks use relatively little pre-processing compared to other image classification algorithms. This means that the network learns to optimize the filters (or kernels) through automated learning, whereas these filters are hand-engineered in traditional algorithms. A significant advantage is an independence from prior knowledge and human intervention in feature extraction.

3.6. Gabor filter and convolutional neural network

The graphical representation of the model is presented in Fig. 4. Fingerprint images are input into two channels, respectively. Channel 1 is a Deep Convolutional Neural Network. The fingerprint image in channel 1 does not need image

typical CNN architecture is shown in Fig. 3, which includes several convolutional and pooling layers. It is based on the shared-weight architecture of the convolution kernels or filters that slide along input features and provide translation-equivariant responses known as feature maps (Zhang et al., 1996).

enhancement, and its features will be fully extracted by the Deep Convolutional Neural Network. Channel 2 is a Shallow Convolutional Neural Network, which requires image enhancement. The output of channel 1 is OUT_{c1} , which is a 128-dimensional vector. The output of channel 2 is OUT_{c2} , which is also a 128-dimensional vector. The OUT_{c1} and OUT_{c2} are concatenated together according to Eq. 9 to obtain OUT , then a 256-dimensional vector is obtained. Finally, pass a fully connected layer and use the Softmax function to get the final output. The model is called Deep Convolutional Neural Network and Shallow Convolutional Neural Network (DCNN-SCNN).

$$OUT = OUT_{c1} \oplus OUT_{c2} \tag{9}$$

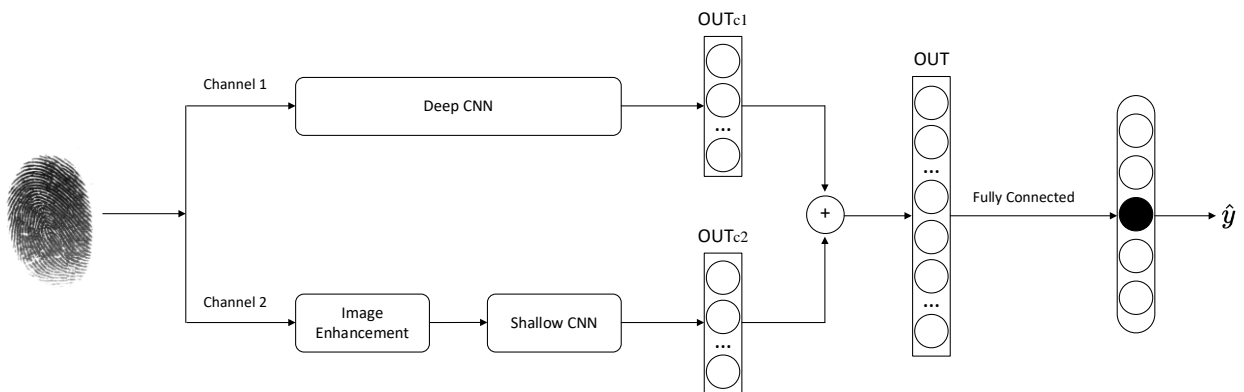


Fig. 4: Overview model

3.7. Deep convolutional neural network

The Deep Convolutional Neural Network (DCNN) consists of an input, hidden, and output layer. In a convolutional neural network, the hidden layers contain layers that perform convolutions. Generally, this contains a layer that performs a dot product of

the convolution kernel with the layer's input matrix. This product is usually the Frobenius inner product, and its activation function is typically ReLU (Agarap, 2018). After the convolutional layer is the pooling layer, the Deep Convolutional Neural Network usually ends with two fully connected layers.

This paper uses a model with eight convolutional layers and two fully connected layers, and the model

parameters are shown in Table 1. This model can extract deep features of the fingerprint.

Table 1: Detailed parameters of the deep CNN model

Layers	Filters	Kernel size	Pool size	Strides	Padding	Shape
Input	-	-	-	-	-	(96, 96, 1)
conv1	64	[5, 5]	-	[1, 1]	SAME	(96, 96, 64)
pooling1	64	-	[3, 3]	[2, 2]	SAME	(48, 48, 64)
conv2	128	[5, 5]	-	[1, 1]	SAME	(48, 48, 128)
pooling2	128	-	[3, 3]	[2, 2]	SAME	(24, 24, 128)
conv3	256	[5, 5]	-	[1, 1]	SAME	(24, 24, 256)
pooling3	256	-	[3, 3]	[2, 2]	SAME	(12, 12, 256)
conv4	512	[5, 5]	-	[1, 1]	SAME	(12, 12, 512)
pooling4	512	-	[3, 3]	[1, 1]	SAME	(12, 12, 512)
conv5	512	[5, 5]	-	[1, 1]	SAME	(12, 12, 512)
pooling5	512	-	[3, 3]	[2, 2]	SAME	(6, 6, 512)
conv6	256	[3, 3]	-	[1, 1]	SAME	(6, 6, 256)
pooling6	256	-	[3, 3]	[2, 2]	SAME	(3, 3, 256)
conv7	128	[3, 3]	-	[1, 1]	SAME	(3, 3, 128)
pooling7	128	-	[3, 3]	[1, 1]	SAME	(3, 3, 128)
conv8	128	[3, 3]	-	[1, 1]	SAME	(3, 3, 128)
pooling8	128	-	[3, 3]	[2, 2]	SAME	(2, 2, 128)
fc1	-	-	-	-	-	(512)
fc2	-	-	-	-	-	(128)

3.8. Shallow convolutional neural network

The fingerprint image needs to be image-enhanced before inputting the Shallow Convolutional Neural Network (SCNN). The fingerprint image enhancement needs to be performed in sequence according to Fig. 5, including

image normalization, orientation field estimation, frequency field estimation, and Gabor filter.

Because the fingerprint image has been enhanced with the Gabor filter, only a Shallow convolutional neural network is needed to complete the fingerprint image feature extraction. The model parameters are shown in Table 2. This model can extract features from clear fingerprint images.

Table 2: Detailed parameters of the shallow CNN model

Layers	Filters	Kernel size	Pool size	Strides	Padding	Shape
Input	-	-	-	-	-	(96, 96, 1)
conv1	64	[5, 5]	-	[1, 1]	SAME	(96, 96, 64)
pooling1	64	-	[3, 3]	[2, 2]	SAME	(48, 48, 64)
conv2	128	[5, 5]	-	[1, 1]	SAME	(48, 48, 128)
pooling2	128	-	[3, 3]	[2, 2]	SAME	(24, 24, 128)
fc1	-	-	-	-	-	(73728)
fc2	-	-	-	-	-	(128)

3.9. Loss function

This paper is a multi-classification problem, so the Softmax function is used. The softmax activation function is often connected after the last layer of the neural network for classification tasks. Compared with Sigmoid, which can only be used for binary classification, Softmax can be used for multi-classification.

Softmax can convert all predicted values into predicted probability values and is constrained to be in the range of [0, 1], and the sum of the probability values is 1. For example, after the predicted value z_i of the i -th category is processed by Softmax, the obtained predicted probability value \hat{y}_i is shown as Eq. 10.

$$\hat{y}_i = \frac{e^{z_i}}{\sum_{j=1}^{|C|} e^{z_j}} \tag{10}$$

In multi-classification tasks, the cross-entropy loss is usually used as the loss function. When using One-Hot encoding, set the batch size to N , then the cross-entropy loss L_{CE} of a batch is shown in Eq. 11.

$$L_{CE} = -\frac{1}{N} \sum_{i=1}^N \log \hat{y}_i \tag{11}$$

In Eq. 11, \hat{y}_i is the predicted probability value. In this paper, the Softmax is added to the last layer of the network, and then the softmax loss is shown in Eq. 12.

$$L_{Softmax} = -\frac{1}{N} \sum_{i=1}^N \log \frac{e^{W_{C_i}^T x_i + b_{C_i}}}{\sum_{j=1}^{|C|} e^{W_j^T x_i + b_j}} \tag{12}$$

3.10. Dataset

Due to fingerprint privacy, this paper uses NIST Special Database 4 for experiments only. This database is valuable for evaluating fingerprint systems on a statistical sample of fingerprints evenly distributed over the five major classifications. NIST Special Database 4 has the following features: 2000 grayscale fingerprint image pairs; 400 fingerprint pairs from each of the five classifications (Right Loop, Left Loop, Whorl, Arch, and Tented Arch); each fingerprint pairs are two completely different rollings of the same fingerprint. Suitable for automated fingerprint classification research, the

database can be used for: algorithm development, system training, and testing (Watson and Wilson, 1992).

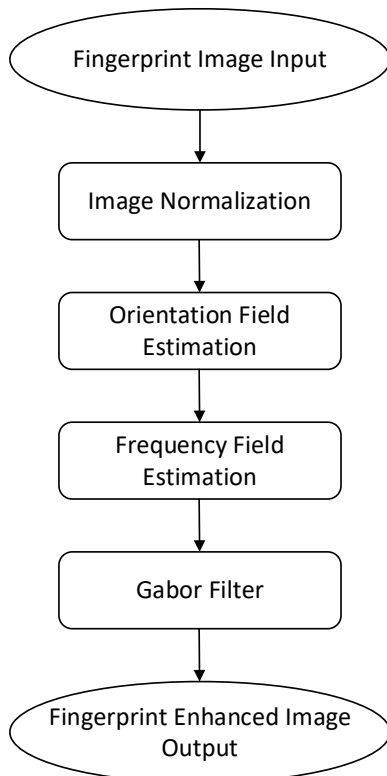


Fig. 5: Fingerprint image enhancement

To effectively verify the accuracy of the model, this paper divides 4000 images of fingerprint data into the training set and the test set according to Table 3. Eight hundred fingerprints of each type (750 for training, 50 for testing). A total of 3750 images for training and 250 images for testing. In order to make the training of the neural network model faster, all fingerprints are resized to 96×96 in this paper.

Table 3: Training set and test set

Type	Training set	Test set	Total
Right Loop	750	50	800
Left Loop	750	50	800
Whorl	750	50	800
Arch	750	50	800
Tented Arch	750	50	800
Total	3750	250	4000

3.11. Fingerprint image enhancement using Gabor filter

In order to apply the Gabor filter to the fingerprint image, three parameters need to be defined:

1. The direction θ of the Gabor filter.
2. The frequency f of the sine plane wave.
3. The standard deviation σ_x and σ_y of the Gaussian envelope.

The direction and frequency of the friction ridges have been calculated. The position of the center of

the filter bandpass region in the frequency domain is determined by f_0 and θ . Different values of σ_x and σ_y will have different effects on the filtered image. The larger their values, the filter's denoising ability is stronger, but the greater the possibility of generating fake friction ridges. This paper sets σ_x and σ_y to 3.8, based on experience and experiments.

This paper uses the method of Fig. 5 to enhance the fingerprint image, and the images before and after enhancement are shown in Table 4. After the fingerprint is enhanced, it will be inputted into the Shallow Convolutional Neural Network model.

Table 4: Images before and after enhancement

Before enhancement	After enhancement

3.12. Model training

This study uses Tensor Flow to create the model and GPU to accelerate the training. The main training parameters of the model are shown in Table 5. This paper trains DCNN-SCNN, DCNN, and SCNN separately under the same parameters.

The training Loss curves of the three models are shown in Fig. 6. As seen from Fig. 6, all three models converge well.

Table 5: Training parameters

Parameters	Value
batch_size	128
training_step	3000
learning_rate	0.0001
Optimizer	Adam optimizer

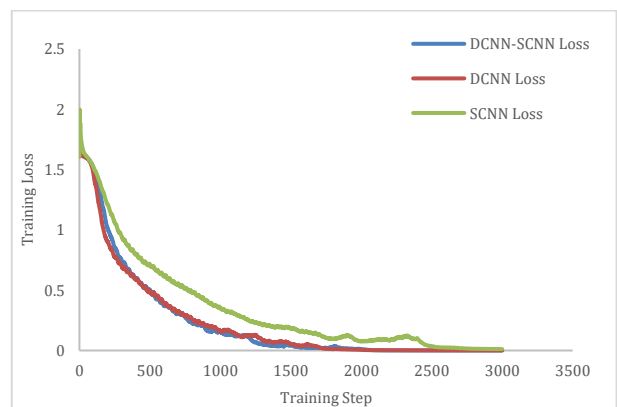


Fig. 6: Training losses of the models

4. Results and discussion

The accuracy of the three models on the test set is shown in Fig. 7. The accuracy of DCNN-SCNN and DCNN are relatively high where DCNN-SCNN can

reach about 0.91 and DCNN can reach about 0.88. The accuracy of SCNN is not as good as that of the others, which can reach about 0.83. The final accuracy of the models using the test set is shown in Table 6.

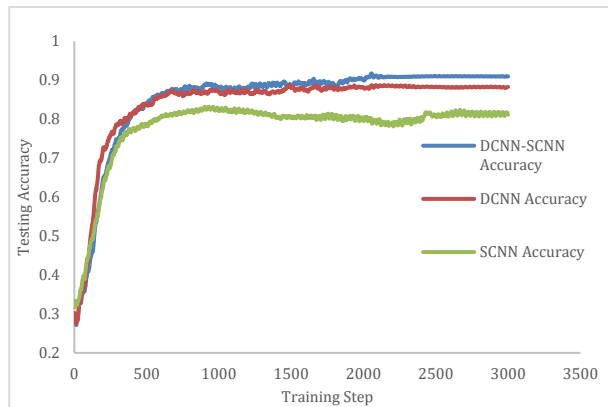


Fig. 7: Test accuracy of the models

Table 6: Final test accuracy of the models

Model name	Final accuracy
SCNN	83.7
DCNN	88.2
DCNN-SCNN	91.4

From Fig. 7 and Table 6, the following information can be obtained:

1. The accuracy of SCNN is the lowest because after the fingerprint is enhanced by the Gabor filter, although clear friction ridges are obtained, some fingerprint details are lost.
2. The accuracy of DCNN-SCNN and DCNN models is close because both models contain Deep Convolutional Neural Networks.
3. The accuracy of DCNN-SCNN is the highest because this model includes DCNN and SCNN. The DCNN can extract the detailed features of the fingerprint, and the fingerprint features extracted by DCNN are closer to the real fingerprint. The SCNN contains Gabor filter, and clear friction ridges can be obtained after the fingerprint is enhanced by the Gabor filter. Consequently, the SCNN can extract clear fingerprint features.

In general, the DCNN-SCNN can extract clear friction ridges fingerprint features and detail fingerprint features hence, the highest accuracy is obtained.

4.1. Comparison with other works

In order to verify the performance of the DCNN-SCNN model, a comparison with the other state-of-the-art models on the NIST Special Database 4 dataset was conducted. The test results and the accuracy of the models are shown in Table 7. Table 7 shows that deep learning algorithms are better than traditional machine algorithms (KNN, RF, SVM) because deep learning algorithms can better extract the detailed features of the fingerprint. The DCNN-SCNN model proposed in this paper has the highest

accuracy among the deep learning algorithms. Since the DCNN-SCNN model has two channels, the clear friction ridges fingerprint features, and detail fingerprint features can be extracted at the same time. It indicates that the DCNN-SCNN model is more effective for the fingerprint classification task.

Table 7: Comparison with other works

Algorithm	Final accuracy
KNN (K-Nearest neighbors)	65.1
RF (Random forest)	72.3
SVM (Support vector machine)	73.7
LCNN and ROI by Jian et al. (2020)	85.5
DCNN	88.2
B-DCNN by Zia et al. (2019)	89.3
Proposed DCNN-SCNN model	91.4

5. Conclusion

This paper first introduces fingerprint and fingerprint classification. The Henry classification system is a widely used system among fingerprint classification systems. Moreover, this study introduces fingerprint image enhancement technology including image normalization, orientation field estimation, frequency field estimation, and Gabor filter. The proposed model has two channels. Channel 1 is a Deep Convolutional Neural Network. The DCNN can extract the detailed features of the fingerprint, and the fingerprint features extracted by DCNN are closer to the real fingerprint. Moreso, Channel 2 is a Shallow Convolutional Neural Network that requires image enhancement. The SCNN contains Gabor filter, and clear friction ridges can be obtained after the fingerprint is enhanced by the Gabor filter. Therefore, the SCNN can extract clear fingerprint features. Furthermore, this paper introduces the experimental process in detail, including the dataset, fingerprint image enhancement, model training, results, and analysis. Experimental results show that the proposed model achieved 91.4% accuracy. Compared with other algorithms, this model obtained higher accuracy than others. Findings show that the combined Gabor filter and Convolutional Neural Network can better extract the ridge features of fingerprint images.

Compliance with ethical standards

Conflict of interest

The author(s) declared no potential conflicts of interest with respect to the research, authorship, and/or publication of this article.

References

- Agarap AF (2018). Deep learning using rectified linear units (ReLU). ArXiv Preprint ArXiv: 1803.08375. <https://doi.org/10.48550/arXiv.1803.08375>
- Cao K, Pang L, Liang J, and Tian J (2013). Fingerprint classification by a hierarchical classifier. Pattern Recognition, 46(12): 3186-3197. <https://doi.org/10.1016/j.patcog.2013.05.008>

- Chang JH and Fan KC (2002). A new model for fingerprint classification by ridge distribution sequences. *Pattern Recognition*, 35(6): 1209-1223.
[https://doi.org/10.1016/S0031-3203\(01\)00121-2](https://doi.org/10.1016/S0031-3203(01)00121-2)
- Chen G, Jiang Z, and Kamruzzaman MM (2020). Radar remote sensing image retrieval algorithm based on improved Sobel operator. *Journal of Visual Communication and Image Representation*, 71: 102720.
<https://doi.org/10.1016/j.jvcir.2019.102720>
- Ding S, Shi S, and Jia W (2020). Research on fingerprint classification based on twin support vector machine. *IET Image Processing*, 14(2): 231-235.
<https://doi.org/10.1049/iet-ipr.2018.5977>
- Faulds H (1880). On the skin-furrows of the hand. *Nature*, 22(574): 605-605. <https://doi.org/10.1038/022605a0>
- Gabor D (1946). Theory of communication. Part 1: The analysis of information. *Journal of the Institution of Electrical Engineers-Part III: Radio and Communication Engineering*, 93(26): 429-441. <https://doi.org/10.1049/ji-3-2.1946.0074>
- Guo JM, Liu YF, Chang JY, and Lee JD (2014). Fingerprint classification based on decision tree from singular points and orientation field. *Expert Systems with Applications*, 41(2): 752-764. <https://doi.org/10.1016/j.eswa.2013.07.099>
- Ibrahim AM, Eesee AK, and Al-Nima RRO (2021). Deep fingerprint classification network. *TELKOMNIKA (Telecommunication Computing Electronics and Control)*, 19(3): 893-901.
<https://doi.org/10.12928/telkomnika.v19i3.18771>
- Jian W, Zhou Y, and Liu H (2020). Lightweight convolutional neural network based on singularity ROI for fingerprint classification. *IEEE Access*, 8: 54554-54563.
<https://doi.org/10.1109/ACCESS.2020.2981515>
- Jiang X (2015). Fingerprint classification. In: Li SZ and Jain AK (Eds.), *Encyclopedia of biometrics*: 584-592. Springer Science and Business Media, Berlin, Germany.
https://doi.org/10.1007/978-1-4899-7488-4_56
- Kanopoulos N, Vasanthavada N, and Baker RL (1988). Design of an image edge detection filter using the Sobel operator. *IEEE Journal of Solid-State Circuits*, 23(2): 358-367.
<https://doi.org/10.1109/4.996>
- Karu K and Jain AK (1996). Fingerprint classification. *Pattern Recognition*, 29(3): 389-404.
[https://doi.org/10.1016/0031-3203\(95\)00106-9](https://doi.org/10.1016/0031-3203(95)00106-9)
- Leung KC and Leung CH (2010). Improvement of fingerprint retrieval by a statistical classifier. *IEEE Transactions on Information Forensics and Security*, 6(1): 59-69.
<https://doi.org/10.1109/TIFS.2010.2100382>
- Li SZ and Jain AK (2015). *Encyclopedia of biometrics*. Springer Science and Business Media, Berlin, Germany.
<https://doi.org/10.1007/978-1-4899-7488-4>
- Moenssens AA (1971). *Fingerprint techniques*. Chilton Book Company, Boston, USA.
- Rao K and Balck K (1980). Type classification of fingerprints: A syntactic approach. *IEEE Transactions on Pattern Analysis and Machine Intelligence*, PAMI-2(3): 223-231.
<https://doi.org/10.1109/TPAMI.1980.4767009>
PMid:21868895
- Rim B, Kim J, and Hong M (2020). Gender classification from fingerprint-images using deep learning approach. In *The International Conference on Research in Adaptive and Convergent Systems*, Association for Computing Machinery, Gwangju, Korea: 7-12.
<https://doi.org/10.1145/3400286.3418237>
- Rim B, Kim J, and Hong M (2021). Fingerprint classification using deep learning approach. *Multimedia Tools and Applications*, 80(28): 35809-35825.
<https://doi.org/10.1007/s11042-020-09314-6>
- Valueva MV, Nagornov NN, Lyakhov PA, Valuev GV, and Chervyakov NI (2020). Application of the residue number system to reduce hardware costs of the convolutional neural network implementation. *Mathematics and Computers in Simulation*, 177: 232-243.
<https://doi.org/10.1016/j.matcom.2020.04.031>
- Wang X, Wang F, Fan J, and Wang J (2009). Fingerprint classification based on continuous orientation field and singular points. In *the 2009 IEEE International Conference on Intelligent Computing and Intelligent Systems*, IEEE, Shanghai, China: 189-193.
<https://doi.org/10.1109/ICICISYS.2009.5357702>
- Watson CI and Wilson CL (1992). NIST special database 4. Fingerprint Database, National Institute of Standards and Technology, 17(77): 5.
- Wu F, Zhu J, and Guo X (2020). Fingerprint pattern identification and classification approach based on convolutional neural networks. *Neural Computing and Applications*, 32(10): 5725-5734. <https://doi.org/10.1007/s00521-019-04499-w>
- Yager N and Amin A (2004). Fingerprint verification based on minutiae features: A review. *Pattern Analysis and Applications*, 7(1): 94-113.
<https://doi.org/10.1007/s10044-003-0201-2>
- Zhang W, Doi K, Giger ML, Nishikawa RM, and Schmidt RA (1996). An improved shift-invariant artificial neural network for computerized detection of clustered microcalcifications in digital mammograms. *Medical Physics*, 23(4): 595-601.
<https://doi.org/10.1118/1.597891> **PMid:8860907**
- Zhengfang H, Delima AJP, Machica IKD, Arroyo JCT, Weibin S, and Gang X (2022). Fingerprint identification based on novel siamese rectangular convolutional neural networks. *International Journal of Emerging Technology and Advanced Engineering*, 12(5): 28-37.
https://doi.org/10.46338/ijetae0522_04
- Zia T, Ghafoor M, Tariq SA, and Taj IA (2019). Robust fingerprint classification with Bayesian convolutional networks. *IET Image Processing*, 13(8): 1280-1288.
<https://doi.org/10.1049/iet-ipr.2018.5466>